DARCY-BRINKMAN FREE CONVECTION FROM A HEATED HORIZONTAL SURFACE

D. A. S. Rees
Department of Mechanical Engineering, University of Bath, Claverton Down, Bath, BA2 7AY, UK

K. Vafai
Department of Mechanical Engineering, Ohio State University, Columbus, Ohio 43210-1107, USA

The free convection boundary layer flow of a Darcy-Brinkman fluid that is induced by a constant-temperature horizontal semi-infinite surface embedded in a fluid-saturated porous medium is investigated in this work. It is shown that both the Darcy and Rayleigh numbers may be scaled out of the boundary layer equations, leaving a parabolic system of equations with no parameters to vary. The equations are studied using both numerical and asymptotic methods. Near the leading edge the boundary layer has a double-layer structure: a near-wall layer, where the temperature adjusts from the wall temperature to the ambient and where Brinkman effects dominate, and an outer layer of uniform thickness that is a momentum-adjustment layer. Further downstream, these layers merge, but the boundary layer eventually regains a two-layer structure; in this case, a growing outer layer exists, which is identical to the Darcy-flow case for the leading order term, and an inner layer of constant thickness resides near the surface, where the Brinkman term is important.

INTRODUCTION

Heat transfer in a saturated porous medium has received considerable attention over the past decades due to its significance in various practical applications. Its application is seen in many geophysical and energy-related problems. Although Darcy's law is commonly used in the calculation of flow and heat transfer features in a saturated porous medium, its validity has been questioned for a wide range of flow regimes and geometries. The objective of this work is to analyze the free convective flow and heat transfer from a heated horizontal surface embedded in a fluid-saturated porous material using the Darcy-Brinkman formulation of the governing equations.

Although the buoyancy-induced flow above a heated horizontal surface has been extensively investigated, the corresponding problem of flow in a saturated

NOMENCLATURE

a	constant	λ	coefficient	
b	constant	μ	dynamic viscosity	
Da	Darcy number	ξ	scaled streamwise coordinate	
f	reduced stream function	ρ	reference fluid density	
F	reduced stream function	σ	unknown coefficient	
$\mathscr{F}$	reduced stream function	ϕ	porosity	
g	scaled temperature	ψ	stream function	
$\hat{g}$	gravitational acceleration			
G	scaled temperature			
$\mathscr{G}$	scaled temperature	**Subscripts**		
K	permeability			
L	macroscopic length scale	max	maximum value for numerical	
$o(X^{-1})$	asymptotically smaller than		solution	
	X^{-1} as $X \to \infty$	L	logarithmic term	
p	pressure	x	differentiation with respect to x	
R	porous medium Rayleigh number	X	differentiation with respect to X	
u	streamwise flux velocity	y	differentiation with respect to y	
v	cross-stream flux velocity	ζ	differentiation with respect to ζ	
x	horizontal or streamwise coordinate	η	differentiation with respect to η	
X	scaled x variable	ξ	differentiation with respect to ξ	
y	vertical or cross-stream coordinate	$0, 1, \ldots$	terms in series expansion	
α	constant given in Eq. (7)			
β	coefficient of thermal expansion	**Superscripts**		
ΔT	temperature range between the			
	wall and the ambient	$^-$	nondimensional (unscaled with	
ζ	similarity variable		respect to α)	
η	similarity variable	$^\wedge$	dimensional	
θ	temperature	$'$	differentiation with respect to	
κ	effective thermal diffusivity		y, η, or ζ	

porous medium adjacent to an impermeable wall has received relatively little attention. Boundary layer approximations similar to those of the classical boundary layer theory have been used because of the existence of a thin thermal boundary layer. However, this boundary layer approximation is a first-order approximation for natural convection at high Rayleigh numbers. The boundary layer analysis neglects higher order effects, such as the entrainments from the edge of the thermal boundary layer, the axial heat conduction, and the normal pressure gradient. Cheng and co-workers [1, 2] used the method of matched asymptotic expansions for the problems of natural convection in a porous medium adjacent to a semi-infinite vertical or horizontal plate with a power law variation of wall temperature. They found that the effects of entrainment from the edge of the thermal boundary layer are of second order, while the axial heat conduction and normal pressure gradient are of third order. The effect of a higher order boundary layer theory was found to be more pronounced on the velocity profiles as compared with the temperature distribution. Cheng and Chang [3] performed a boundary layer analysis for the buoyancy-induced flows in a saturated porous medium adjacent to horizontal impermeable surfaces. They obtained similarity solutions for the convective flow above a heated surface and below a cooled surface and

obtained analytical expressions for the boundary layer thickness and the local and overall surface heat flux. Kim and Vafai [4] analyzed in detail the buoyancy-driven flow and heat transfer about a vertical flat plate embedded in a porous medium. The governing equations were solved analytically using the method of matched asymptotic expansions, and they also obtained a numerical solution based on the similarity transformation. It was found that the heat transfer rate is proportional to the Rayleigh number for the case when the thermal boundary layer thickness is larger than that of the viscous boundary layer. On the other hand, the heat transfer rate was found to be proportional to the product of the Rayleigh number and the porosity when the thickness of the viscous boundary layer is larger.

A primary objective of this paper is to determine how boundary friction affects the free convective flow pattern in a porous medium. The evolution of the structure of the boundary layer along the edge of the heated horizontal surface will be studied. An analytical solution is obtained by scaling both the Darcy and Rayleigh numbers out of the boundary layer equations. The importance of the Brinkman term at different axial locations along the plate is also investigated.

EQUATIONS OF MOTION AND BOUNDARY LAYER ANALYSIS

Consider the free convective boundary layer flow induced by a constant-temperature-heated horizontal surface embedded in a fluid-saturated porous medium. In this paper we will assume that the surface is upward facing, that the Oberbeck-Boussinesq approximation is valid, that the solid matrix and the saturating fluid are in local thermal equilibrium, and that the flow is governed by the Darcy-Brinkman equations supplemented by the energy transport equation. The resulting flow is two-dimensional and steady (in the absence of destabilizing disturbances) and is therefore governed by the following set of nondimensional equations (see [4]):

$$\frac{\partial \hat{u}}{\partial \hat{x}} + \frac{\partial \hat{v}}{\partial \hat{y}} = 0 \tag{1a}$$

$$\hat{u} = -\frac{\partial \hat{p}}{\partial \hat{x}} + \mathrm{Da}\,\nabla^2 \hat{u} \tag{1b}$$

$$\hat{v} = -\frac{\partial \hat{p}}{\partial \hat{y}} + \mathrm{Da}\,\nabla^2 \hat{v} + R\hat{\theta} \tag{1c}$$

$$\hat{u}\frac{\partial \hat{\theta}}{\partial \hat{x}} + \hat{v}\frac{\partial \hat{\theta}}{\partial \hat{y}} = \nabla^2 \hat{\theta} \tag{1d}$$

Here $\hat{x}$ and $\hat{y}$ are Cartesian coordinates oriented along and perpendicular to the heated surface (with $\hat{x} = 0$ corresponding to the leading edge), $\hat{u}$ and $\hat{v}$ are the corresponding fluid flux velocities, $\hat{p}$ is the pressure, and $\hat{\theta}$ is the temperature of the saturated medium. On the heated surface, which is situated at $\hat{y} = 0$ and $\hat{x} \geqslant 0$, the temperature is $\hat{\theta} = 1$, whereas $\hat{\theta} \to 0$ far from the surface. The two nondimensional parameters that appear in Eq. (1) are the Darcy and Rayleigh

numbers, which are defined respectively as

$$Da = \frac{K}{L^2\phi} \quad Ra = \frac{\rho\hat{g}\beta K L\,\Delta T}{\mu\kappa} \tag{2}$$

The various terms introduced in Eq. (2) have their usual meanings: K is the permeability, L a macroscopic length scale, ϕ the porosity, ρ a reference fluid density, $\hat{g}$ gravitational acceleration, β the volumetric expansion coefficient, ΔT the temperature drop between the heated surface and the ambient fluid, μ the viscosity, and κ the thermal diffusivity. A stream function may be introduced in the usual way: $\hat{u} = \hat{\psi}_{\hat{y}}$, $\hat{v} = -\hat{\psi}_{\hat{x}}$, and we obtain the following pair of equations:

$$\nabla^2\hat{\psi} = -Ra\,\hat{\theta}_{\hat{x}} + Da\nabla^4\hat{\psi} \tag{3a}$$

$$\nabla^2\hat{\theta} = \hat{\psi}_{\hat{y}}\hat{\theta}_{\hat{x}} - \hat{\psi}_{\hat{x}}\hat{\theta}_{\hat{y}} \tag{3b}$$

which are to be solved subject to the boundary conditions:

$$\hat{\psi} = \hat{\psi}_{\hat{y}} = 0 \qquad \hat{\theta} = 1 \qquad \hat{y} = 0 \qquad \hat{x} \geqslant 0 \qquad \hat{\psi}_{\hat{y}}, \hat{\psi}_{\hat{y}\hat{y}}, \hat{\theta} \to 0 \qquad \hat{y} \to \infty \tag{4}$$

Both Ra and Da appear in Eqs. (3a), and although it is possible to eliminate both parameters at this stage by means of suitable resealings, it is preferable to set the following analysis into the context of the well-known Darcy-flow study of Cheng and Chang [3], where boundary frictional effects were assumed to be absent. Thus we use the traditional scalings for horizontal free convection boundary layer flow in a porous medium and set

$$\hat{\psi} = Ra^{1/3}\,\overline{\psi} \qquad \hat{\theta} = \overline{\theta} \qquad \hat{x} = \overline{x} \qquad \hat{y} = Ra^{-1/3}\,\overline{y} \tag{5}$$

where we also take Ra to be asymptotically large. Substitution of Eq. (5) into Eqs. (3a) and (3b) yields the following equations:

$$\overline{\psi}_{\overline{y}\overline{y}} = -\overline{\theta}_{\overline{x}} + \alpha\overline{\psi}_{\overline{y}\overline{y}\overline{y}\overline{y}} \tag{6a}$$

$$\overline{\theta}_{\overline{y}\overline{y}} = \overline{\psi}_{\overline{y}}\overline{\theta}_{\overline{x}} - \overline{\psi}_{\overline{x}}\overline{\theta}_{\overline{y}} \tag{6b}$$

at leading order in Ra. Here we have α defined as

$$\alpha = Da\,Ra^{2/3} \tag{7}$$

and if we can assume at this stage that this quantity is $O(1)$ as $Ra \to \infty$, then it implies that $Da \ll 1$ in magnitude, which is physically realistic.

When $\alpha = 0$ in Eq. (6a), Eqs. (6a) and (6b) comprise the boundary layer equations for Darcy-free convection. But when $\alpha \neq 0$, we can rescale again and

eliminate α from the equations. This is done by substituting

$$\bar{\psi} = \alpha^{1/4}\psi \qquad \bar{\theta} = \theta \qquad \bar{x} = \alpha^{3/4}x \qquad \bar{y} = \alpha^{1/2}y \qquad (8)$$

into Eqs. (6 a) and (6 b), and therefore we obtain

$$\psi_{yy} = -\theta_x + \psi_{yyyy} \qquad (9a)$$

$$\theta_{yy} = \psi_y\theta_x - \psi_x\theta_y \qquad (9b)$$

Finally, before the boundary layer analysis is undertaken, it is essential to check that the boundary layer approximation has not been violated by imposing the second transformation, Eq. (8). Thus we require $\hat{x} \gg \hat{y}$ for the approximation to be valid, and this implies that $\mathrm{Ra} \gg O(\mathrm{Da}^{-1/2})$. It should be noted that in ref. [4] the two physical cases in terms of the interplay between the momentum and thermal boundaries are analyzed in detail and analytical solutions are obtained for both constant temperature as well as constant heat flux boundary conditions.

ASYMPTOTIC ANALYSIS FOR SMALL VALUES OF x

A straightforward scale analysis shows that the appropriate similarity form close to the leading edge is obtained by using

$$\psi = x^{3/5}F(\zeta, X) \qquad \theta = G(\zeta, X) \qquad \zeta = y/x^{2/5} \qquad X = x^{2/5} \qquad (10)$$

which, upon substitution in Eqs. (9 a) and (9 b) leads to

$$F_{\zeta\zeta\zeta} + \tfrac{2}{5}\zeta G_\zeta - X^2 F_{\zeta\zeta} = \tfrac{2}{5}XG_X \qquad (11a)$$

$$G_{\zeta\zeta} + \tfrac{3}{5}FG_\zeta = \tfrac{2}{5}X(F_\zeta G_X - F_X G_\zeta) \qquad (11b)$$

The boundary conditions at $\zeta = 0$ are that $F = F_\zeta = 0$ and $G = 1$, and we expect that $G \to 0$ as $\zeta \to \infty$. The ordinary differential system, which is obtained by setting $X = 0$ in Eqs. (11 a) and (11 b) cannot be solved using the boundary conditions $F_\zeta, F_{\zeta\zeta} \to 0$ as $\zeta \to \infty$, which correspond to the large-$\hat{y}$ conditions on ψ, which are given in Eq. (4). However, a solution is easily found if the large-ζ conditions are replaced by $F_{\zeta\zeta}, F_{\zeta\zeta\zeta} \to 0$. In this case, we find that F varies linearly at sufficiently large values of ζ, rather than being a constant. Thus the requirement that $F_\zeta \to 0$ is violated. We will see, however, that this is accounted for by invoking the presence of an outer, "momentum-adjustment" layer.

This outer layer corresponds to where $y = O(1)$ as $x \to 0$ (noting that $y = O(x^{2/5})$ in the main thermal boundary layer). Given that $F_\zeta \to a_0$, a constant, as $\zeta \to \infty$, it is clear from Eq. (11 b) that G exhibits superexponential decay for large values of ζ when $X = 0$, for G becomes proportional to $\exp(-(3/10)a_0\zeta^2)$. Therefore the temperature field is negligible in the outer layer, and we can introduce the following transformation for ψ in the outer layer:

$$\psi = x^{1/5}\mathscr{F}(y, x) \qquad (12)$$

Equation (9 a) reduces to

$$\mathcal{F}_{yyyy} - \mathcal{F}_{yy} = 0 \tag{13}$$

where the matching conditions at $\zeta = 0$ and the boundary conditions as $\zeta \to \infty$ are

$$\mathcal{F} = 0 \qquad \mathcal{F}_y = a_0 \quad \text{at} \quad y = 0, \qquad \mathcal{F}_y, \mathcal{F}_{yy} \to 0 \quad \text{as} \quad y \to \infty \tag{14}$$

The solution for $\mathcal{F}$ is

$$\mathcal{F} = a_0(1 - e^{-y}) \tag{15}$$

The solution Eq. (15) is the leading term in the outer layer solution for small values of x. It is possible to proceed to quite a large number of terms in both the outer and main layers with the application of suitable matching conditions between the layers. To summarize the result of this process, which is quite straightforward, we can expand F and G in Eqs. (11 a) and (11 b) and $\mathcal{F}$ in Eq. (13) using the following series:

$$(F, G) = \sum_{n=0}^{\infty} X^n [F_n(\zeta), G_n(\zeta)] \tag{16a}$$

$$\mathcal{F} = \sum_{n=0}^{\infty} X^n \mathcal{F}_n(y) \tag{16b}$$

The equations for the various coefficient functions are

$$F_0'''' + \tfrac{2}{5}\zeta G_0' = 0 \qquad G_0'' + \tfrac{3}{5}F_0 G_0' = 0 \tag{17}$$

$$F_1'''' + \tfrac{2}{5}(\zeta G_1' - G_1) = 0 \qquad G_1'' + \tfrac{3}{5}(F_0 G_1' + F_1 G_0') = \tfrac{2}{5}(F_0' G_1 - F_1 G_0') \tag{18}$$

$$F_n'''' + \tfrac{2}{5}(\zeta G_n' - n G_n) = F_{n-2}'' \qquad G_n'' + \tfrac{3}{5}\sum_{i=0}^{n} F_i G_{n-i}' = \tfrac{2}{5}\sum_{i=1}^{n}(F_{n-i}' G_i - F_i G_{n-i}')$$

$$n = 2, 3, \ldots, \tag{19}$$

$$\mathcal{F}_n''' - \mathcal{F}_n'' = 0 \qquad n = 0, 1, \ldots, \tag{20}$$

The large-ζ behavior of the F_n functions in the inner layer is

$$F_0 \sim (a_0 \zeta + b_0) \tag{21a}$$

$$F_1 \sim -\frac{1}{2!}a_0 \zeta^2 + (a_1 \zeta + b_1) \tag{21b}$$

$$F_2 \sim \frac{1}{3!}a_0 - \frac{1}{2!}a_1 \zeta^2 + (a_2 \zeta + b_2) \tag{21c}$$

$$F_3 \sim -\frac{1}{4!}a_0 + \frac{1}{3!}a_1 - \frac{1}{2!}a_2 \zeta^2 + (a_3 \zeta + b_3) \tag{21d}$$

and so on, with the constants a_n and b_n being found when solving the appropriate equations for F_n and G_n. The outer solutions are, simply,

$$\mathscr{F}_0 = a_0(1 - e^{-y}) \qquad \mathscr{F}_n = b_{n-1} + a_n(1 - e^{-y}) \qquad n = 1, 2, \ldots, \qquad (22)$$

The values of a_n and b_n that appear in Eqs. (21) and (22) are given in Table 1 for the first six terms in the series solution. They were calculated using a fourth-order Runge-Kutta scheme linked to the shooting method, where ζ ranged between 0 and 20 with 1600 equally spaced intervals; these solutions are accurate as shown in the table, and comparisons were made with coarser grids and larger values of ζ_{max}. The inner solutions obtained are presented in Figure 1 in terms of the various temperature profiles. The surface shear stress and rate of heat transfer may be found by using

$$\left.\frac{\partial^2 F}{\partial \zeta^2}\right|_{\zeta=0} = \sum_{n=0} X^n F_n''(0) \qquad \left.\frac{\partial G}{\partial \zeta}\right|_{\zeta=0} = \sum_{n=0} X^n G_n'(0) \qquad (23)$$

together with the data in the final two columns of Table 1. The values of the surface shear stress and rate of heat transfer given in Eq. (23) are plotted in Figure 2 together with the results of the full numerical simulation described below.
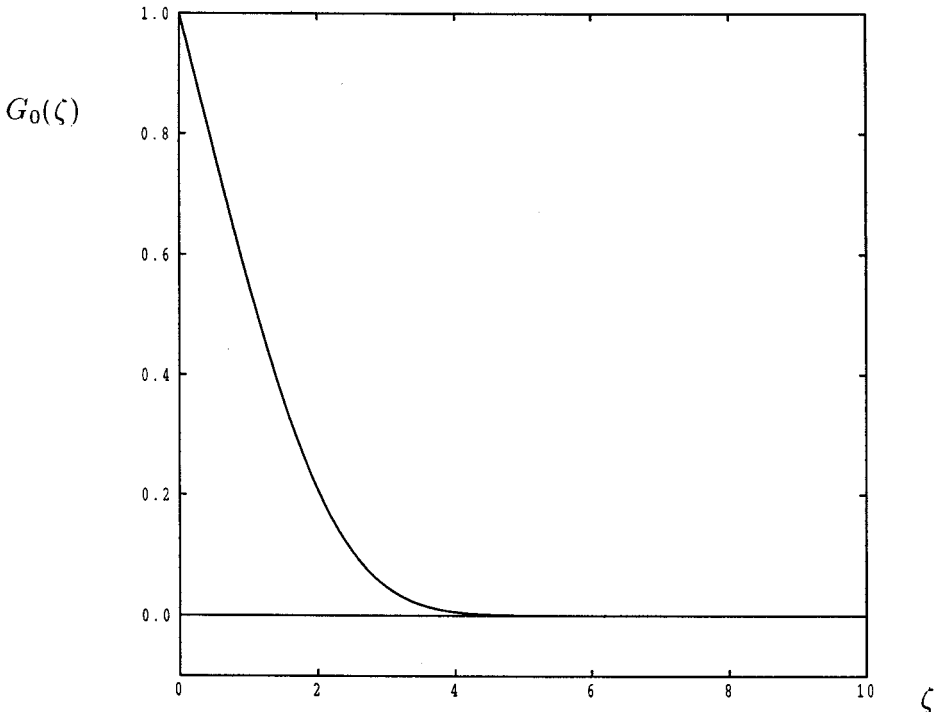

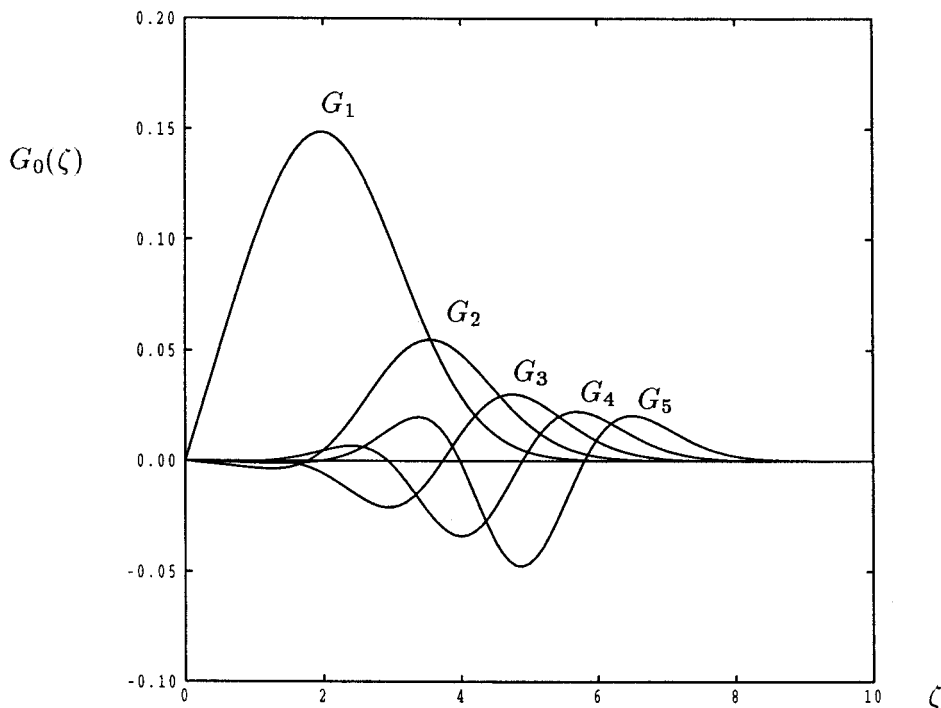**Figure 1 a.** $G_0(\zeta)$ as obtained by solving Eq. (17).

Figure 1 b. $G_n(\zeta)$ $(n = 1, \ldots, 5)$ as obtained by solving Eqs. (18) and (19).

ASYMPTOTIC ANALYSIS FOR LARGE VALUES OF x

Far from the leading edge, we revert to the Darcy-flow similarity form and use

$$\psi = x^{1/3} f(\eta, \xi) \qquad \theta = g(\eta, \xi) \qquad \eta = y/x^{2/3} \qquad \xi = x^{4/3} \tag{24}$$
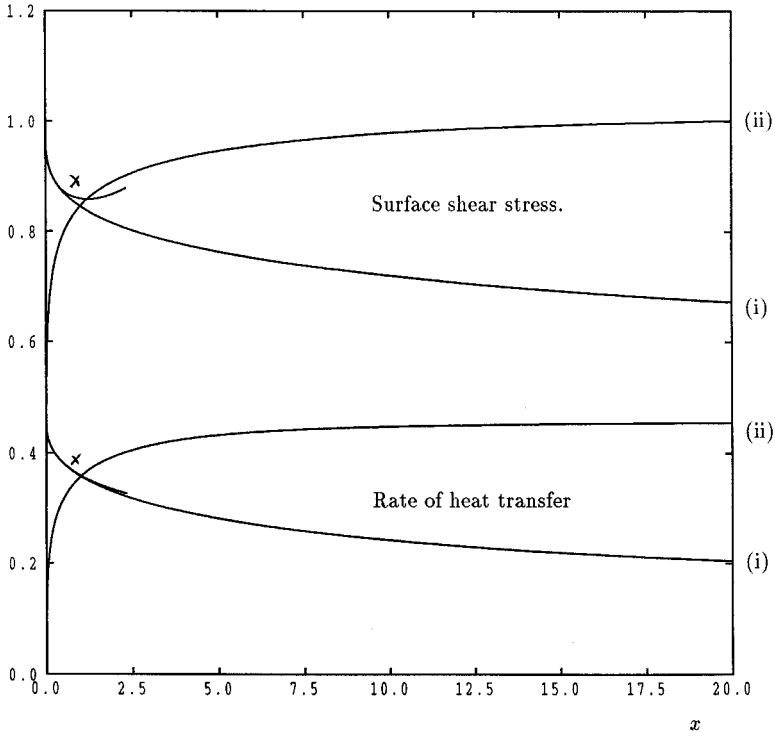
in Eqs. (9a) and (9b) to obtain

$$f_{\eta\eta} - \tfrac{2}{3}\eta g_\eta - \xi^{-1} f_{\eta\eta\eta\eta} = -\tfrac{4}{3}\xi g_\xi \tag{25a}$$

$$g_{\eta\eta} + \tfrac{1}{3} f g_\eta = \tfrac{4}{3}\xi(f_\eta g_\xi - f_\xi g_\eta) \tag{25b}$$

Table 1. Values of a_n, b_n, $F_n''(0)$, and $G_n'(0)$

n	a_n	b_n	$F_n''(0)$	$G_n'(0)$
0	1.1488	− 1.0392	− 0.97534	− 0.45619
1	1.7233	− 2.1230	− 0.15296	1.0291×10^{-1}
2	2.4621	− 3.2583	6.5140×10^{-4}	-3.2358×10^{-3}
3	3.3729	− 4.5410	2.1878×10^{-2}	-3.6892×10^{-4}
4	4.5293	− 6.1284	1.4068×10^{-2}	-5.9935×10^{-4}
5	6.0474	− 8.2238	5.5784×10^{-4}	-9.4625×10^{-4}

Figure 2. Surface shear stress and rate of heat transfer given by (i) Eqs. (51 a) and (ii) Eqs. (51 b). Also shown are the corresponding results obtained from the small-x asymptotic analysis.

subject to

$$f = 0 \qquad f_{\eta} = 0 \qquad g = 1 \qquad \eta = 0 \qquad f_{\eta}, f_{\eta\eta}, g \to 0 \qquad \eta \to \infty \qquad (26)$$

A straightforward expansion of Eqs. (25a) and (25b) in an inverse power series in ξ shows that the fourth derivative term in Eq. (25a) is negligible at leading order and therefore the large-ξ analysis is a singular perturbation problem with two layers appearing again. Therefore we need to install a relatively thin layer near the surface, where η is very small. This inner layer must have $y = O(1)$ in order to balance the momentum terms in Eq. (25a). Therefore we rewrite Eqs. (25a) and (25b) using the transformations

$$f(\eta, \xi) = \mathscr{F}(y, \xi) \qquad g(\eta, \xi) = \mathscr{G}(y, \xi) \qquad (27)$$

and hence we obtain

$$\mathscr{F}_{yy} - \mathscr{F}_{yyyy} + \tfrac{4}{3}\mathscr{G}_{\xi} = 0 \qquad (28\,a)$$

$$\mathscr{G}_{yy} + \tfrac{1}{3}\xi^{-1/2}\mathscr{F}\mathscr{G}_{y} = \tfrac{4}{3}\xi^{1/2}(\mathscr{F}_{y}\mathscr{G}_{\xi} - \mathscr{F}_{\xi}\mathscr{G}_{y}) \qquad (28\,b)$$

We have used the same notation for this constant-thickness inner layer as we used for the outer layer near $x = 0$; this is because these respective layers are of the same uniform thickness. The presence of the $\xi^{1/2}$ terms in Eqs. (28a) and (28b) suggests that the solutions of Eqs. (25) and (28) proceed in inverse powers of $\xi^{1/2}$. However, the $O(\xi^{-1/2})$ equations in the expansion of Eqs. (25a) and (25b) admit eigensolutions and are insoluble. Therefore logarithmic terms must be introduced: let

$$f = f_0(\eta) + f_{1L}(\eta)\xi^{-1/2} \ln \xi + f_1(\eta)\xi^{-1/2} + \cdots \qquad (29a)$$

$$g = g_0(\eta) + g_{1L}(\eta)\xi^{-1/2} \ln \xi + g_1(\eta)\xi^{-1/2} + \cdots \qquad (29b)$$

in Eqs. (25a) and (25b), where

$$f_0'' - \tfrac{2}{3}\eta g_0' = 0 \qquad g_0'' + \tfrac{1}{3}f_0 g_0' = 0 \qquad (30)$$

$$f_{1L}'' - \tfrac{2}{3}(\eta g_{1L}' + g_{1L}) = 0 \qquad g_{1L}'' + \tfrac{1}{3}(f_0 g_{1L}' - f_{1L} g_0' + 2 f_0' g_{1L}) = 0 \qquad (31)$$

$$f_1'' - \tfrac{2}{3}(\eta g_1' + g_1) = \tfrac{4}{3}g_{1L} \qquad g_1'' + \tfrac{1}{3}(f_0 g_1' - f_1 g_0' + 2 f_0' g_1) = \tfrac{4}{3}(f_0' g_{1L} - f_{1L} g_0')$$

$$\qquad (32)$$

In the inner layer the expansion begins as follows,

$$\mathscr{F} = \mathscr{F}_0(y) + \mathscr{F}_1(y)\xi^{-1/2} + \mathscr{F}_{2L}\xi^{-1} \ln \xi + \mathscr{F}_2 \xi^{-1} + \cdots \qquad (33a)$$

$$\mathscr{G} = \mathscr{G}_0(y) + \mathscr{G}_1(y)\xi^{-1/2} + \mathscr{G}_{2L}\xi^{-1} \ln \xi + \mathscr{G}_2 \xi^{-1} + \cdots \qquad (33b)$$

and the boundary conditions are that

$$\mathscr{F}_0(0) = \mathscr{F}_0'(0) = 0 \qquad \mathscr{G}_0(0) = 1 \qquad (34a)$$

and

$$\mathscr{F}_n(0) = \mathscr{F}_n'(0) = \mathscr{G}_n(0) = 0 \qquad n = 1, 2, \ldots \qquad (34b)$$

with suitable matching conditions between the layers as $y \to \infty$ and $\eta \to 0$.

   The solution of Eqs. (30) subject to $f_0(0) = 0$, $g_0(0) = 1$, and f_0', $g_0 \to 0$ as $\eta \to \infty$ is well-known and was first presented by Cheng and Chang [3]. The small-η behavior of f_0 and g_0 must be examined to provide matching conditions for the inner layer solutions:

$$f_0(\eta) = a\eta + \tfrac{1}{9}b\eta^3 + \cdots \qquad g_0(\eta) = 1 + b\eta - \tfrac{1}{18}ab\eta^3 + \cdots \qquad (35)$$

where $a = 1.055748$ and $b = -0.430213$ to six decimal places. Therefore we deduce that the first two terms in the inner layer solution are

$$\mathscr{F}_0(y) = 0 \qquad \mathscr{G}_0(y) = 1 \qquad (36)$$

and

$$\mathscr{F}_1(y) = a(e^{-y} - 1 + y) \tag{37a}$$

$$\mathscr{G}(y) = by \tag{37b}$$

The "-1" term in Eq. (37a) provides a forcing term for the $O(\xi^{-1/2})$ outer layer solution via the matching conditions. Therefore Eqs. (31) and (32) must be solved subject to the boundary conditions

$$f_{1L}(0) = 0 \qquad g_{1L}(0) = 0 \qquad f_{1L}, g_{1L} \to 0 \qquad \eta \to \infty \tag{38}$$

$$f_1(0) = -a \qquad g_1(0) = 0 \qquad f_1, g_1 \to 0 \qquad \eta \to \infty \tag{39}$$

The solution of Eqs. (31) subject to Eqs. (38) is the eigensolution

$$f_{1L} = \lambda(\eta f_0' - f_0) \qquad g_{1L} = \lambda \eta g_0' \tag{40}$$

where λ is presently unknown but its value is determined by insisting that Eqs. (32) have a solution. The solution to Eqs. (32) may be written in the form

$$f_1 = \sigma(\eta f_0' - f_0) - f_0' + b f_{1\dagger} \qquad g_1 = \sigma \eta g_0' - g_0' + b g_{1\dagger} \tag{41}$$

where $f_{1\dagger}$ and $g_{1\dagger}$ satisfy the equations

$$f_{1\dagger}'' - \tfrac{2}{3}(\eta g_{1\dagger}' + g_{1\dagger}) = \tfrac{4}{3}\lambda \eta g_0' \qquad g_{1\dagger}'' + \tfrac{1}{3}(f_0 g_{1\dagger}' - f_{1\dagger} g_0' + 2 f_0' g_{1\dagger}) = \tfrac{4}{3}\lambda f_0 g_0' \tag{42}$$

subject to the boundary conditions

$$f_{1\dagger}(0) = 0 \qquad g_{1\dagger}(0) = 1 \qquad f_{1\dagger}, g_{1\dagger} \to 0 \qquad \eta \to \infty \tag{43}$$

We note that Eqs. (42) cannot be solved with λ set to zero, i.e., in the absence of logarithmic terms in Eqs. (29a) and (29b). Now σ is an arbitrary constant in Eq. (41), and its precise value may only be found by comparing the boundary layer solution with a solution of the full elliptic equations of motion. Numerically, it is necessary to choose an arbitrary value for σ in order to obtain a solution of Eqs. (41), and therefore we shall set $g_{1\dagger}'(0) = 0$. This fifth boundary condition for Eqs. (42) enables us to evaluate λ, but the choice of the fifth boundary condition does not affect the computed value of λ. We find that

$$\lambda = -0.149516 \qquad f_{1\dagger}'(0) = -0.469567 \tag{44}$$

The $O(\xi^{-1} \ln \xi)$ and $O(\xi^{-1})$ solutions in the inner layer are now

$$\mathscr{F}_{2L} = 0 \qquad \mathscr{G}_{2L} = \lambda by \tag{45}$$

$$\mathscr{F}_2 = b f_{1\dagger}'(0) y \qquad \mathscr{G}_2 = \sigma by \tag{46}$$

Therefore we may summarize these various results in terms of the surface shear stress and rate of heat transfer:

$$\mathscr{F}_{yy}|_{y=0} = a\xi^{-1/2} + o(\xi^{-1}) \tag{47a}$$

$$\mathscr{G}_{y}|_{y=0} = b\xi^{-1/2} + \lambda b\xi^{-1} \ln \xi + b\sigma\xi^{-1} + (\xi^{-1}) \tag{47b}$$

In terms of f, g, and η (see Eqs. (24)), the above translates into

$$f_{\eta\eta}|_{\eta=0} = a\xi^{1/2} + o(1) \tag{48a}$$

$$g_{\eta}|_{\eta=0} = b + \lambda b\xi^{-1/2} \ln \xi + b\sigma\xi^{-1/2} + o(\xi^{-1/2}) \tag{48b}$$

NUMERICAL SOLUTIONS

Equations (11) (used for $X \leqslant 1$ or $x \leqslant 1$) and Eqs. (25) (used for $\xi \geqslant 1$ or $x \geqslant 1$) form a parabolic system of equations whose solution may be affected by means of a marching scheme such as the Keller box method [5], which has been used for boundary layer flows. The present system of equations poses a novel difficulty for the application of the method, as the boundary layer has a double-layer structure near the leading edge, where the computations must be initiated. Normally, a double-layer structure, should one exist, develops as x becomes large, but this poses little difficulty (apart from resolution), as the development is gradual. It is quite possible, however, to mimic the double-layer structure near the leading edge in the present problem by a suitably modified set of boundary conditions. The small-x outer flow solutions given by Eqs. (22) are all of the form $\mathscr{F} = B + Ae^{-y}$, and this may be rewritten in terms of ζ as $\mathscr{F} = B + Ae^{-\xi\zeta}$. This exponential decay to a constant value of the scaled stream function, together with the linear growth of F_0 (see Eq. (21a)) at $x = 0$, may be combined by solving Eqs. (11a) and (11b) subject to the boundary conditions

$$F = 0 \qquad F_\zeta = 0 \qquad G = 1 \qquad \zeta = 0 \tag{49a}$$

$$(F_{\zeta\zeta} + \xi F_\zeta), (F_{\zeta\zeta\zeta} + \xi F_{\zeta\zeta}), G \rightarrow 0 \qquad \zeta \rightarrow \infty \tag{49b}$$

The imposition of the conditions in F in Eq. (49b) means that F_ζ will not necessarily be close to zero at $\zeta = \zeta_{\max}$, the maximum value of ζ used in the computational work, but the exponential decay corresponding to the outer layer is assured. As ξ increases, the rate of decay increases too, and eventually, F_ζ at $\zeta = \zeta_{\max}$ will be sufficiently small (say, 10^{-6}), that we can revert to the following large-ζ conditions:

$$F_\zeta, F_{\zeta\zeta}, G \rightarrow 0 \qquad \zeta \rightarrow \infty \tag{50}$$

It is necessary that the switch between the large-ζ conditions given in Eq. (49b) and those in Eq. (50) be made as soon as possible as ξ increases, and therefore quite a large value of $\zeta_{\max}$ must be used. In the present computation, $\zeta_{\max} = 200$ was used, which is well in excess of that essential for the accurate solution of F_0 and G_0 (Eqs. (17)), and therefore the switch between the boundary conditions may be made before ξ reaches 0.1. We note that this technique of using modified

boundary conditions to account for an outer flow regime has also been used successfully in the recent paper by Rees and Pop [6].

The standard Keller box method was used to solve the governing parabolic partial differential system. Briefly, Eqs. (11) and (25) were reduced to first-order form in either ζ or η and discretized using central differences based halfway between the grid points on a nonuniform cross-stream grid of 97 points with $0 < \zeta, \eta < 200$. Grid points were concentrated toward the surface in order to capture the developing near-wall layer far from the leading edge. The streamwise discretization was based on central differences except at the leading edge, where Eqs. (11) result in an ordinary differential system. In the streamwise direction, we used a nonuniform grid of 186 points between 0 and 100. The Newton-Raphson iteration matrix, which forms the central part of the Keller box method was computed numerically within the code, rather than specified by the programmer; see also Refs. [6]-[8]. As Eqs. (11) and (13) do not contain any nondimensional parameters to vary, the code needed only to be run once to obtain all the required information about the effects of boundary friction on horizontal free convection flow.

The numerical results are presented in terms of the surface shear stress and the rate of heat transfer, as shown in Figure 2. This information is presented in two forms: (i)

$$
\begin{array}{lll}
F_{\zeta\zeta}|_{\zeta=0} & - G_{\zeta}|_{\zeta=0} & x \leqslant 1 \qquad \text{and} \\
x^{-4/5} f_{\eta\eta}|_{\eta=0} & - x^{-4/15} g_{\eta}|_{\eta=0} & x \geqslant 1
\end{array}
\tag{51 a}
$$

which is suitable for small values of x where the quantities are nonzero at $x = 0$, and (ii)

$$
\begin{array}{lll}
x^{2/15} F_{\zeta\zeta}|_{\zeta=0} & - x^{4/15} G_{\zeta}|_{\zeta=0} & x \leqslant 1 \qquad \text{and} \\
x^{-2/3} f_{\eta\eta}|_{\eta=0} & - g_{\eta}|_{\eta=0} & x \geqslant 1
\end{array}
\tag{51 b}
$$

which is suitable for large values of x where both quantities tend toward nonzero constants as x becomes large. Cross-validation of the Keller box computation and the small-x analysis is seen in Figure 2, where the agreement between the two analyses is very good. At large values of x it is clear that the presence of the unknown constant, σ, in the asymptotic solution reduces substantially the usefulness of that solution in providing accurate values of the shear stress and rate of heat transfer. Although we have determined two terms explicitly for the surface rate of heat transfer, the third term, which involves σ, has an order of magnitude that is smaller than the second by a factor $(\ln \xi)^{-1}$, and therefore it decays very slowly as ξ increases.

DISCUSSION

The primary purpose of this paper was to determine in detail how boundary friction effects in the form of the Brinkman terms affect the classical Cheng and Chang [3] horizontal free convective boundary layer flow in a porous medium. It has been shown that the boundary layer consists of a double-layer structure very near to the leading edge. The outer layer here may be regarded as a momentum

adjustment layer, since the inner layer is dominated by boundary frictional effects. These layers merge as x increases, and the numerical method had to be carefully tailored to account for the presence of the outer layer very near the leading edge. However, as x increases further, a double-layer structure is recovered, the outer layer being identical to the Darcy-flow case given in Ref. [1], at least to the leading order. The inner layer is dominated by boundary frictional effects that modify the flow near the surface but not the rate of heat transfer.

It is of some interest to point out that the outer layer for small values of x and the inner layer at large values of x are of the same uniform thickness, since both are described in terms of the nondimensional cross-stream variable y. This thickness, namely, $y = O(1)$, corresponds to $\hat{y} = O(\text{Da}^{1/2})$, which corresponds exactly to a balance of magnitudes between the velocity flux term and the Brinkman term in Eqs. (1b) and (1c). Clearly, $\hat{y} = O(\text{Da}^{1/2})$ is a natural length scale in problems where boundary frictional effects occur. In terms of y, the evolving thermal boundary layer is much thinner than $O(1)$ at the leading edge (its thickness is $O(x^{2/5})$ for small values of x) and is much thicker than $O(1)$ far downstream (where its thickness is $O(x^{2/3})$ for large values of x). It should be noted that in this work, the inertial and dispersion effects as well as non-local thermal equilibrium and variable porosity effects were neglected based on the results presented in refs [9] to [11].

REFERENCES

1. I. D. Chang and P. Cheng, Matched Asymptotic Expansions for Free Convection About an Impermeable Horizontal Surface in a Porous Medium, *Int. J. Heat Mass Transfer*, vol. 26, pp. 163−174, 1983.
2. P. Cheng and C. T. Hsu, Higher-Order Approximations for Darcian Free Convection About a Semiinfinite Vertical Flat Plate, *J. Heat Transfer*, vol. 106, pp. 143−151, 1984.
3. P. Cheng and I. D. Chang, On Buoyancy Induced Flows in a Saturated Porous Medium Adjacent to Impermeable Horizontal Surfaces, *Int. J. Heat Mass Transfer*, vol. 19, pp. 1267−1272, 1976.
4. S. J. Kim and K. Vafai, Analysis of Natural Convection About a Vertical Plate Embedded in a Porous Medium, *Int. J. Heat Mass Transfer*, vol. 32, pp. 665−677, 1989.
5. H. B. Keller and T. Cebeci, Accurate Numerical Methods for Boundary Layer Flows: 1 —Two dimensional Flows, Proc. Int. Conf. Numerical Methods in Fluid Dynamics, *Lecture Notes in Physics*, Springer, New York, 1971.
6. D. A. S. Rees and I. Pop, Vertical Free Convection Boundary Layer Flow in a Porous Medium Using a Thermal Nonequilibrium Model, to appear, *J. Porous Media*, 1998.
7. D. A. S. Rees, Free Convective Boundary Layer Flow from a Heated Surface in a Layered Porous Medium, in press, *J. Porous Media*, 1998.
8. D. A. S. Rees and I. Pop, Free Convection Induced by a Horizontal Wavy Surface in a Porous Medium, *Fluid Dyn. Res.*, vol. 14, pp. 151−166, 1994.
9. J. Ettefagh, K. Vafai and S. J. Kim, Non-Darcian Effects in Open-Ended Cavities Filled with a Porous Medium, *ASME J. Heat Transfer*, vol. 113, pp. 747−756, 1991.
10. A. Amiri and K. Vafai, Analysis of Dispersion Effects and Non-Equilibrium, Non-Darcian, Variable Porosity Incompressible Flow Through Porous Media, *Int. J. Heat Mass Transfer*, vol. 37, pp. 939−954, 1994.
11. C. L. Tien and K. Vafai, Convective and Radiative Heat Transfer in Porous Media, *Advances in Applied Mechanics*, vol. 27, pp. 225−281, 1989.